ASTROPHYSICAL JOURNAL LETTERS, SUBMITTED
Preprint typeset using LaTeX style emulateapj v. 14/09/00

THE SUPER STAR CLUSTER NGC 1569-A RESOLVED ON SUB-PARSEC SCALES WITH *HUBBLE SPACE TELESCOPE* SPECTROSCOPY[1]

DAN MAOZ[2,3], LUIS C. HO[4], AND AMIEL STERNBERG[3]

Received 2001 May 1; Accepted May 22

ABSTRACT

We present 3000–10000 Å *HST*/STIS long-slit spectroscopy of the bright super star cluster A (SSC-A) in the dwarf starburst galaxy NGC 1569. The 0.″05 *HST* angular resolution allows, for the first time, to probe for spatial variations in the stellar population of a $\sim 10^6 M_\odot$ SSC. Integrated ground-based spectra of SSC-A have previously revealed young Wolf-Rayet (WR) signatures that coexist with features from supposedly older, red supergiant (RSG), populations. We find that the WR emission complexes come solely from the subcluster A2, identified in previous *HST* imaging, and are absent from the main cluster A1, thus resolving the question of whether the WR and RSG features arise in a single or distinct clusters. The equivalent widths of the WR features in A2 — including the C IV λ5808 complex which we detect in this object for the first time — are larger than previously observed in other WR galaxies. Models with sub-solar metallicity, as inferred from the nebular emission lines of this galaxy, predict much lower equivalent widths. On the "clean" side of A1, opposite to A2, we find no evidence for radial gradients in the observed stellar population at $0.''05 < R < 0.''40$ (~ 0.5 to 5 pc), neither in broad-band, low-resolution, spectra nor in medium-resolution spectra of the infrared Ca II triplet.

Subject headings: galaxies: individual (NGC 1569) — galaxies: star clusters — galaxies: starburst — galaxies: stellar content — stars: Wolf-Rayet

1. INTRODUCTION

A substantial fraction of the star formation in nearby starbursts, be it in merging galaxies, dwarf galaxies, or early-type galaxies with circumnuclear rings, takes place in so-called super star clusters (SSCs; e.g., Whitmore et al. 1999; Hunter et al. 2000; Maoz et al. 2001, and references therein). These are clusters of stars with total luminosities as high as $M_V = -15$ mag ($L_V = 1.3 \times 10^8 L_{V\odot}$) and radii of order a few pc. SSCs present a mode of massive star formation distinct from the OB associations found in most star-forming regions of quiescent galaxies. They are of interest for understanding star formation at high redshift, which is dominated by the starburst mode, and the formation of globular clusters, into which SSCs may evolve if they contain sufficient numbers of low-mass stars, and can survive disruption and evaporation.

Two of the nearest (2.5 ± 0.5 Mpc; O'Connell, Gallagher, & Hunter 1994) and best-studied SSCs are clusters A and B in the amorphous dwarf galaxy NGC 1569 (Arp & Sandage 1985; Melnick, Moles, & Terlevich 1985). NGC 1569-A is one of only several SSCs that have a kinematic mass estimate, $\approx 10^6 M_\odot$ (Ho & Filippenko 1996; Sternberg 1998). Prada, Greve, & McKeith (1994) detected the Ca II $\lambda\lambda 8498, 8542, 8662$ absorption triplet, which forms in the atmospheres of red giants and supergiants, in cluster A. Based on the equivalent width (EW) of these lines, they estimated an age > 13 Myr. González Delgado et al. (1997), however, detected in the SSC-A spectrum the bump around 4686 Å generally ascribed to He II, C III, C IV, N III, and N V emission from Wolf-Rayet (WR) stars. WR stars are the evolved stages of stars more massive than $\sim 30 M_\odot$, and are thought to exist only when a burst is $3-5$ Myr old. To explain this, González Delgado et al. (1997) proposed that there have been several succesive bursts of star formation in SSC-A. De Marchi et al. (1997) analyzed post-refurbishment *Hubble Space Telescope (HST)* images and showed that SSC-A has two peaks in its light distribution, separated by 0.″18, which they designated A1 and A2, and postulated that these are two distinct clusters, with the WR features coming from one cluster and the red supergiant signatures from the other. More recently, Hunter et al. (2000) obtained deeper *HST* images in several bands, and argued against the proposed solution of De Marchi et al. (1997), based on the finding that A1 and A2 have similar colors. They noted that WR stars and red supergiants are expected to co-exist, to some degree, when a cluster is about 5 Myr old. Nonetheless, Buckalew et al. (2000) have found evidence, based on *HST* He II narrow-band imaging, that the WR emission is concentrated in A2.

More generally, how SSCs form and survive as bound objects is an unsolved problem, given the rapid ejection of gas from the proto-clusters by jets, ionizing radiation, stellar winds, and subsequent supernovae. Some clues may be found in the spatial structure of the nearest SSCs. NGC 3603 in the Milky Way and R136 in the Large Magellanic Cloud (LMC) show some evidence for segregation of the stellar population, with the most massive stars concentrated at smaller radii (Moffat, Drissen, & Shara 1994; Brandl et al. 1996; Hunter et al. 1996). It is thought that the clusters are too young for dynamical mass segregation to have occurred (Bonnell & Davies 1998). The segregation therefore may reflect a gradient in age or in initial mass function (IMF) properties, but could also be a statistical effect, due to the rarity of high-mass stars in the outer, low stellar-density regions of the clusters. Current estimates for the masses of these clusters are $\sim 10^4 - 10^5 M_\odot$ (Drissen et al. 1995). The spatial population profile of massive, $10^6 M_\odot$ SSCs such as NGC 1569-A has never been observed. This Letter presents resolved *HST* long-slit spectroscopy of NGC 1569-A

[1] Based on observations made with the *Hubble Space Telescope*, which is operated by AURA, Inc., under NASA contract NAS5-26555.

[2] Department of Astronomy, Columbia University, 550 W. 120th St., New York, NY 10027; dani@wise.tau.ac.il
[3] School of Physics & Astronomy, Tel-Aviv University, Tel-Aviv 69978, Israel; amiel@wise.tau.ac.il
[4] The Observatories of the Carnegie Institution of Washington, 813 Santa Barbara St., Pasadena, CA 91101; lho@ociw.edu

to address several of these issues.

2. OBSERVATIONS AND REDUCTION

We observed NGC 1569 on 28 November 2000 UT, using the Space Telescope Imaging Spectrograph (STIS) on *HST* . The $52'' \times 0\farcs1$ slit was centered on SSC-A, and the spacecraft was oriented with the intention that clusters A1 and A2, and cluster B, $7''$ to the south-east, would all fall within the narrow slit. Unfortunately, a $0\fdg45$ error in the header orientation information of a WFPC2 image of the galaxy from 1996, combined with a $0\fdg33$ error in determination of the STIS slit orientation in the focal plane at the time the observation was planned, resulted in a total orientation error of $0\fdg78$. The $0\farcs1$-wide slit was misplaced $0\farcs1$ southwest from the center of SSC-B, effectively missing it. A repeat observation of SSC-B is planned, and in this Letter we will analyze only the spectra of SSC-A.

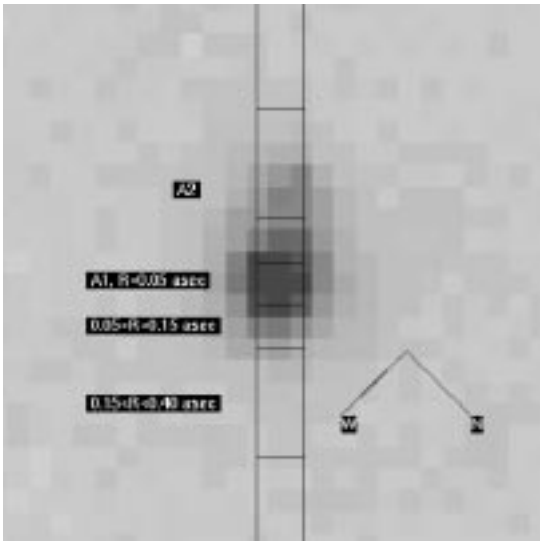

Fig. 1– Section ($1\farcs15 \times 1\farcs15$) of STIS acquisition image of NGC 1569-A. The slit position is shown, and the various spatial bins for which spectra were extracted are labeled.

Exposure times totaled 32.4 min in the G750L grating (5250–10250 Å, 10 Å resolution full width at half maximum [FWHM]), 43.2 min in the G430L grating (2910–5714 Å, 5.5 Å resolution), and 93.6 min in the G750M grating (8276–8842 Å, 1.1 Å resolution). The STIS plate scale is $0\farcs05$ pixel^{-1}. Flat-field exposures were taken with the G750L and G750M gratings for use in fringe correction. The data were initially processed by the STScI pipeline, producing geometrically corrected, flux- and wavelength-calibrated two-dimensional spectral images at each of three dither positions. The fringe flats were normalized and then scaled to give the best suppression of the fringing in the science images. The images at the individual dither positions were registered and combined. Spectra of each of the resolved spatial bins of SSC-A were then obtained by summing individual rows. The five spatial bins chosen were a central bin, consisting of the two rows with peak flux ($R < 0\farcs05$), two intermediate-radius bins, each consisting of two rows above and below the central bin ($0\farcs05 < R < 0\farcs15$), and two outer bins ($0\farcs15 < R < 0\farcs40$). The outer bin on the south-east side of SSC-A is dominated by flux from SSC-A2, while the center and north-west bins are dominated by flux from SSC-A1. Figure 1 shows the location of the rectangular sections of SSC-A we have thus probed.

Despite the geometric correction applied to the data in the pipeline, some residual curvature remains in the spectral images. Combined with the unavoidable variations in point-spread function (PSF) along the large wavelength interval of the low-resolution spectra, this produces conspicuous artificial spectral variations between different rows. To correct for these effects, we obtained the G430L and G750L archival data of two white dwarfs, GRW+70D5824 and Feige 110, respectively, which were observed with the same STIS setup. We simulated an A1+A2 cluster pair having *no* spatial color gradient by convolving the spectral images of the stars with Gaussians, scaling, shifting, and adding the images, according to the widths and relative fluxes measured in WFPC2 images by Hunter et al. (2000). We verified that the cross-dispersion profile at 5500 Å of the simulated data matched closely that of the real data, which have FWHM of $0\farcs20 \pm 0\farcs02$. We then extracted spectra in the same spatial bins as above, normalized by the total spectrum of the simulated cluster. The resulting correction function was heavily smoothed to eliminate residual spectral features from the white dwarfs, and each spatial bin in the real data was divided by its corresponding correction function. The correction functions are insensitive, at a level of a few percent or less, to the details of the simulation, as long as it includes 2 sources with approximately the correct scaling and the total profile has $0\farcs15 < \mathrm{FWHM} < 0\farcs27$.

Background emission from the sky and from the galaxy in the neighborhood of the cluster is negligible. To obtain a "clean" spectrum of A2, the spectrum of the A1 bin diametrically opposed to it was subtracted from the A2 bin. Residual cosmic rays and bad pixels in the final spectra were identified by eye and corrected by interpolation between adjacent pixels. There is agreement in slope and flux level between the G430L and G750L spectra in the overlap region at 5250 Å to 5714 Å to the few-percent level, except for the central bin spectra, where the G430L spectrum must be scaled up by 15% to match the G750L data. After accounting for the 40% transmission of the total light by the $0\farcs1$ slit, the total SSC-A flux matches well the measurements by González Delgado et al. (1997) and De Marchi et al. (1997).

3. ANALYSIS AND DISCUSSION

3.1. *Subcluster A2 and the Wolf-Rayet Emission*

Figure 2 shows the final low-resolution spectra for each of the spatial bins. To allow easy comparison of the spectral shapes, the spectra have been multiplicatively scaled up to match the central-bin spectrum in the blue region, and then shifted up or down by an additive constant. The spectrum of the A2 bin is shown before subtraction of the northwest, diametrically-opposed, bin of A1 (NW $0\farcs15 < R < 0\farcs40$). The EWs of the main emission and absorption features are listed in Table 1.

González Delgado et al. (1997) first reported the WR emission bump at 4686 Å in the integrated spectrum of SSC-A. It is clear from Figure 2 that this feature, as well as the strong C IV λ5808 Å WR complex which we identify for the first time in this object, come almost exclusively from SSC-A2. Indeed, the weakness or absence of the WR features in the A1 bins demonstrates the angular resolving power of this observation. These results resolve the issue of the co-existence, in SSC-A, of WR with red supergiant signatures, confirming the interpretation proposed by De Marchi et al. (1997) and the narrow-band imaging results of Buckalew et al. (2000). It is unknown whether, at the $0\farcs18$ (2.2 pc) separation, A2 is a separate cluster

seen in projection, or rather a physical neighbor or substructure to A1. In either case, the data show that A2 constitutes a distinct stellar population. Note that, apart from the WR features in A2, the stronger Balmer-line emission in A2, and a possible difference in the spectral shape at $\lambda < 3600$ Å, the spectra of A1 and A2 are quite similar. This confirms and explains the observation by Hunter et al. (2000) of similar optical colors in A1 and A2.

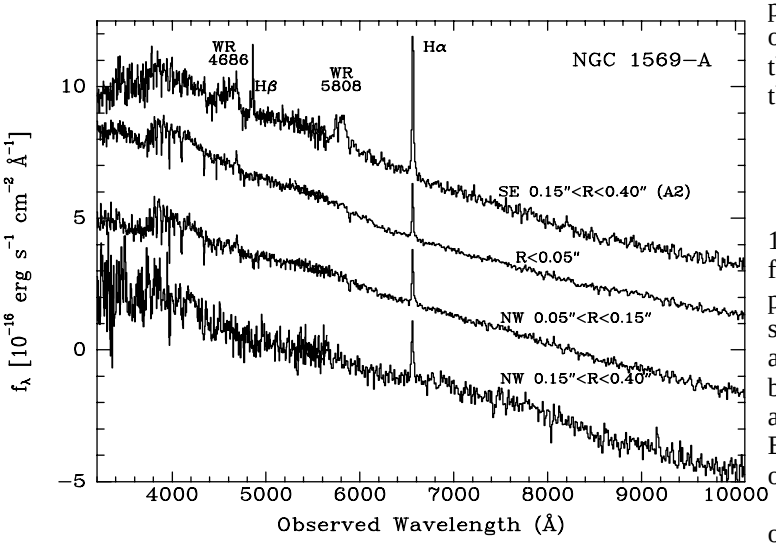

Fig. 2– Broad-band spectra for each of the spatial bins of NGC 1569-A. The flux scale corresponds to the second spectrum from the top (the central, $R < 0\farcs05$, bin of A1). Note the strong WR emission that comes almost exclusively from the A2 bin, and the similarity of the continuum shape among all bins. Scaling and shifting that has been applied to the spectra, from top to bottom, is $2.5 f_\lambda + 2.2 \times 10^{-16}$; $f_\lambda + 0$; $2.25 f_\lambda - 3.5 \times 10^{-16}$; and $5.6 f_\lambda - 6.5 \times 10^{-16}$.

The flux in the 4686 Å feature is consistent with the measurement by González Delgado et al. (1997), who concluded it requires the luminosity of 20–40 WNL stars. However, now that this emission is localized to the relatively faint sub-clump A2, the EW of the WR features becomes huge. After subtraction of the background from A1, we measure EW(4686)=33±9 Å and EW(5808)=32±9 Å. For comparison, Schaerer, Contini, & Kunth (1999) have measured in five WR galaxies typical values of EW(4686)=4–10 Å and EW(5808)=2–6 Å. They find the highest values, with EW(5808)∼ 12 Å, in the galaxy Tol 89. Schaerer & Vacca (1998) have constructed evolutionary synthesis models for instantaneous starbursts and predicted the strengths of the WR features as a function of starburst age and metallicity. As seen, for example, in Figure 11 of Schaerer & Vacca (1998), the WR emission peaks briefly between ages of 3–5 Myr, and its strength is proportional to the metallicity Z. For $Z = 0.2 Z_\odot$, they predict that the EW of either of the WR bumps never rises above 8 Å, and for $Z = 0.4 Z_\odot$, it has a maximum of 11 Å. Only at $Z = 2 Z_\odot$ do the EWs ever reach EW(4686)=30 Å and EW(5808)=25 Å.

However, several measurements of the gas chemical abundances in NGC 1569 have yielded a significantly sub-solar metallicity, of $Z \approx 0.25 Z_\odot$ (Calzetti, Kinney, & Storchi-Bergmann 1994; Kobulnicky & Skillman 1997; González Delgado et al. 1997). The large EWs of the WR features we find in A2 would therefore indicate that, contrary to the line-emitting gas from which they were recently formed, the stars in A2 have solar or supersolar abundances. Alternatively, there may be a problem with the models, in that the WR lifetimes depend on uncertain mass-loss rates and the effects of stellar rotation (Maeder & Meynet 2000). Note that, in a non-instantaneous starburst, the EW of the WR features will necessarily be smaller, thus exacerbating the problem. If A2 is not a separate cluster, or a subcluster of A, but rather a particular physical region of cluster A, then it is not clear that subtraction of the A1 background is justified. In that case, the EWs (and the errors) of the WR features are halved, but are still double the values expected for the metallicity of the gas.

3.2. *Cluster A1 Population and Radial Color Gradient*

The data for the "clean," northwest, side of SSC-A1 in Fig. 1 reveal the spectrum of A1, uncontaminated by A2. We defer a detailed analysis and comparison with models to a future paper. However, except for the WR features which we have shown come from A2, the main characteristics of the spectrum are unchanged in comparison to the integrated spectra analyzed by previous ground-based studies (e.g., González Delgado et al. 1997). Specifically, the blue slope and the weakness of the Balmer jump still point to an age of ~ 5 Myr, and the presence of the Ca II triplet absorption rules out a younger age.

It is remarkable that A1 and A2 appear to have similar ages of ~ 5 Myr, but that one has WR emission and the other does not. A possible explanation is that A1 has an IMF with an upper cutoff $\lesssim 30 M_\odot$, and therefore does not form WR stars. A higher mass cutoff in A2 could be related to its anomalously high metallicity, suggested by the large EWs of its WR features. Alternatively, A1 may also have high, approximately solar, metallicity, but is slightly older than A2, say ~ 7 Myr, by which time it would have exited its WR phase (Schaerer & Vacca 1998). Finally, A1 may have the normal, sub-solar metallicity of the galaxy, in which case it would just be exiting its WR phase already at 5 Myr. Thus A1 and A2 must have widely different IMFs, or widely different abundances, or similar, anomalously high, abundances but slightly different ages.

The northwest A1 data also allow us to examine, for the first time, the radial gradient in the stellar population of an individual high-mass SSC. As seen in Figure 2, there is remarkable similarity in the spectra of A1 in the three radial bins shown. This indicates that, at least on its northwest side, A1 is extremely homogeneous. Considering the small age, the formation of stars in A1 must have been highly synchronized throughout its volume. In this respect, SSC-A1 appears to differ from other, lower mass, SSCs that possibly do show population segregation (see §1).

3.3. *Calcium Triplet Spectra*

Figure 3 shows a region of the medium-resolution G750M spectra centered on the near-infrared Ca II triplet. The spectra of the outer bins are too noisy to reveal unambiguously the Ca II triplet, and are not shown. Figure 3 and Table 1 show that there is no significant difference in Ca II triplet absorption between the central and intermediate radial bins in SSC-A1. This result confirms the lack of a population gradient seen in the low-resolution, broad-band spectra. Although the strength of the Ca II triplet absorption, which comes first from red supergiants and at a later stage from red giants, has been used to

argue for a large age for SSC-A (Prada et al. 1994), the data are also consistent with an age of ~ 5 Myr. García-Vargas, Mollan, & Bressan (1998) have used evolutionary synthesis models to predict the EW for the sum of the two strongest triplet lines, at 8542 Å and 8662 Å. The summed EW value seen in NGC 1569, of $\sim$3–5 Å, is generally lower than the value predicted for starbursts older than 6 Myr, regardless of metallicity (cf. Böker et al. 2001 for caveats on the accuracy of the low-metallicity models). The observed EW, on the other hand, briefly matches the model predictions for cluster ages 5–6 Myr, when the red supergiants first form.

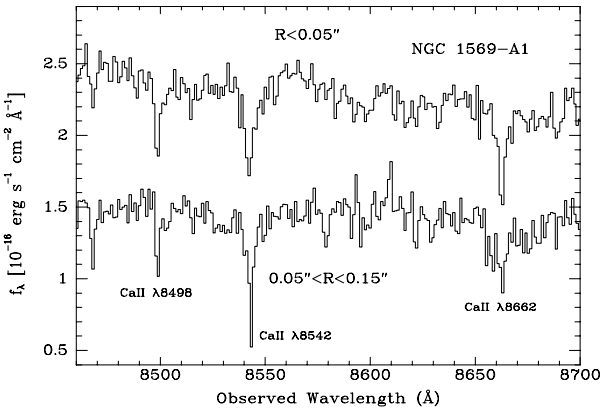

Fig. 3– Medium-resolution spectra centered on the near-infrared Ca II triplet absorption. The lower spectrum, which is the sum of the spectra of the two bins straddling the central bin, has been shifted down by 0.8 units. Note the similarity of Ca II triplet absorption strength at the different radii.

3.4. *Summary*

We have obtained spectra of NGC 1569-A that are resolved at the sub-pc scale, the first time a $10^6 M_\odot$ SSC is observed this way. The data clearly show that the WR emission from this SSC is confined to subcluster A2. The EWs of the WR features are much larger than previously observed in other WR galaxies, and are several times larger than the maximum values predicted from models with sub-solar metallicities, as measured in the gas of this galaxy. This problem is particularly severe if A2 is a separate structure (as opposed to a region inside A1), justifying the subtraction of the underlying light of A1 from A2. The continuum slope, the Balmer jump, the Ca II absorption and WR emission EWs, are all consistent with an age of ~ 5 Myr for the bursts that formed both A1 and A2. While there is a sharp difference in WR population between A1 and A2, there is no significant spatial gradient in the stellar population on the NW side of A1.

We conclude that, either A2 has an anomalous, super-solar metal abundance, or the models have seriously underpredicted the WR emission strength for sub-solar metallicities. The weakness of WR features in A1, despite the similar age to A2, could be caused by a much lower IMF upper-mass cutoff in A1, a much lower metallicity in A1, or a slightly larger age for A1. Finally, the homogeneity of A1 is distinct from the possible radial mass segregation reported in some lower mass SSCs in the Galaxy and the LMC. Further analysis is required to determine the degree to which the apparent uniformity may be set by the most massive stars, which dominate the light. If real, it needs to be reproduced by models of SSC formation and evolution.

This work was supported by grant GO-8293 from the Space Telescope Science Institute, which is operated by AURA, Inc., under NASA contract NAS 5-26555.

TABLE 1
NGC 1569-A: EMISSION AND ABSORPTION EQUIVALENT WIDTHS

	A2	A1		
		$R<0\farcs05$	$0\farcs05<R<0\farcs15$	$0\farcs15<R<0\farcs40$
H$\delta\lambda$4102	-0.5 ± 0.5	-2.8 ± 0.4	-3.0 ± 0.7	-1 ± 1
H$\gamma\lambda$4340	1.2 ± 0.8	-2.0 ± 0.3	-2.5 ± 0.5	-2 ± 1
WR λ4686	33 ± 9	1.9 ± 0.5	1.1 ± 0.5	<1.5
H$\beta\lambda$4861	11 ± 1	-0.3 ± 0.1	-0.9 ± 0.3	0 ± 1
WR λ5808	32 ± 9	<3	<3	<8
H$\alpha\lambda$6563	56 ± 6	8.8 ± 0.5	8.5 ± 1.0	10 ± 2
Ca II λ8498	···	-1.1 ± 0.2	-0.9 ± 0.2	···
Ca II λ8542	···	-2.4 ± 0.6	-1.5 ± 0.5	···
Ca II λ8662	···	-1.7 ± 0.5	-1.7 ± 0.6	···

Note. — Equivalent widths in Å. Positive values are for emission and negative for absorption. WR denotes the broad Wolf-Rayet emission complexes roughly centered on the wavelengths listed. Errors correspond to $\sim 2\sigma$ and are dominated by continuum placement uncertainty.

REFERENCES

Arp, H., & Sandage, A. 1985, AJ, 90, 1163
Böker, T., van der Marel, R. P., Mazzuca, L., Rix, H.-W., Rudnick, G., Ho, L. C., & Shields, J. C. 2001, AJ, 121, 1473
Bonnell, I.A., & Davies, M.B. 1998, MNRAS, 295, 691
Brandl, B., et al. 1996, ApJ, 466, 254
Buckalew, B. A., Dufour, R. J., Shopbell, P. L., & Walter, D. K. 2000, AJ, 120, 2402
Calzetti, D., Kinney, A. L. & Storchi-Bergmann, T. 1994, ApJ, 429, 582
De Marchi, G., Clampin, M., Greggio, L., Leitherer, C., Nota, A., & Tosi, M. 1997, ApJ, 479, L27
Drissen, L., Moffat, A. F. J., Walborn, N. R., & Shara, M. M. 1995, AJ, 110, 2235
García-Vargas, M. L., Molla, M., & Bressan, A. 1998, A&AS, 130, 513
González Delgado, R. M., Leitherer, C., Heckman, T., & Cerviño, M. 1997, ApJ, 483, 705
Ho, L. C., & Filippenko, A. V. 1996, ApJ, 466, L83
Hunter, D. A., O'Connell, R. W., & Gallagher, J. S. 1994, AJ, 108, 84
Hunter, D. A., O'Connell, R. W., Gallagher, J. S. & Smecker-Hane, T. A. 2000, AJ, 120, 2383
Hunter, D. A., O'Neil, E. J., Lynds, R., Shaya, E. J., Groth, E. J., & Holtzman, J. A. 1996, ApJ, 459, L27
Kobulnicky, H. A. & Skillman, E. D. 1997, ApJ, 489, 636
Maeder, A. & Meynet G. 2000, ARAA 38, 143
Maoz, D., Barth, A. J., Ho, L. C., Sternberg, A., & Filippenko, A. V. 2001, AJ, in press ((astrop-ph/0103213)
Melnick, J., Moles, M., & Terlevich, R. 1985, A&A, 149, L24
Moffat, A. F. J., Drissen, L., & Shara, M. M. 1994, ApJ, 436, 183
O'Connell, R. W., Gallagher, J. S., & Hunter, D. A. 1994, ApJ, 433, 65
Prada, F., Greve, A., & McKeith, C. D. 1994, A&A, 288, 396
Schaerer, D., Contini, T., & Kunth, D. 1999, A&A, 341, 399
Schaerer, D. & Vacca, W. D. 1998, ApJ, 497, 618
Sternberg, A. 1998, ApJ, 506, 721
Whitmore, B. C., Zhang, Q., Leitherer, C., Fall, S. M., Schweizer, F. & Miller, B. W. 1999, AJ, 118, 1551